

# RSC Advances



This is an *Accepted Manuscript*, which has been through the Royal Society of Chemistry peer review process and has been accepted for publication.

*Accepted Manuscripts* are published online shortly after acceptance, before technical editing, formatting and proof reading. Using this free service, authors can make their results available to the community, in citable form, before we publish the edited article. This *Accepted Manuscript* will be replaced by the edited, formatted and paginated article as soon as this is available.

You can find more information about *Accepted Manuscripts* in the [Information for Authors](#).

Please note that technical editing may introduce minor changes to the text and/or graphics, which may alter content. The journal's standard [Terms & Conditions](#) and the [Ethical guidelines](#) still apply. In no event shall the Royal Society of Chemistry be held responsible for any errors or omissions in this *Accepted Manuscript* or any consequences arising from the use of any information it contains.

## COMMUNICATION

# New Insight into the Photo-induced Electron Transfer with a Simple Ubiquinone-based Triphenylamine Model

Cite this: DOI: 10.1039/x0xx00000x

Xiao-Yuan Liu, Yi-Tao Long\* and He Tian

Received 00th January 2012,

Accepted 00th January 2012

DOI: 10.1039/x0xx00000x

www.rsc.org/

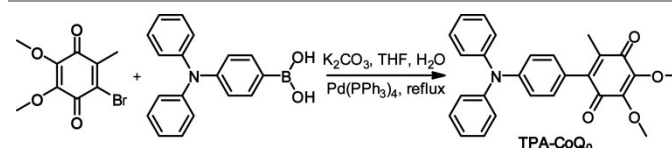
**A ubiquinone-based triphenylamine compound (TPA-CoQ<sub>0</sub>) was synthesized as a simple model to study the photo-induced electron transfer (PET), where the redox processes of ubiquinone could switch the off/on fluorescent of TPA-CoQ<sub>0</sub>/TPA-H<sub>2</sub>CoQ<sub>0</sub> via controlling the reversibly PET processes. The Density Functional Theory (DFT) studies indicated that the switched PET processes rely on the matched molecular orbitals of TPA group and CoQ<sub>0</sub>/H<sub>2</sub>CoQ<sub>0</sub> moiety. This work provides a simple model to deeper understand the PET process and a guide for designing new PET-based molecules in the future.**

In photosynthesis process, photo-induced electron from excited state of P<sub>680</sub> in photosystem II (PSII) is transferred along an electron transport chain accompanying with the proton transfer via three mobile carriers (plastoquinone, plastocyanin and ferredoxin) to fulfil the synthesis process of adenosine triphosphate (ATP) and the reduction of carbon dioxide, where the photo-induced electron transfer (PET) plays an essential role resulting in high photoconversion quantum yield.<sup>1-3</sup> Inspired by nature, great of efforts have been done based on the PET in chemistry<sup>4-10</sup>, biochemistry<sup>11-13</sup> and materials<sup>14-16</sup>, attempting to construct a biomimetic model to understand the PET process in photosystem II and develop artificial photosynthesis systems with high energy-conversion efficiency like photosynthesis.<sup>17-19</sup> In consideration of the key role of quinone in photosynthesis and its prototypical reversible redox property, quinone-based PET systems have also been designed as artificial photosynthesis systems<sup>20, 21</sup> and fluorescence sensors<sup>22-25</sup> to obtain an increasingly clear picture of PET process. In these systems, quinone, as an electron acceptor, captures the electron from the photoexcited electron donor or controls the switched fluorescent via its redox property. The PET process was used for explaining the experimental results in these works, but it lacks the fundamental studies from the nature of molecules. From photosynthesis and the previous works, it is clear that suitable molecular systems are essential for realizing

efficient PET process. However, it is scarce to understand the quinone-based PET process from molecular basis and explore a simple molecular model to guide molecular design because the reported systems are too complex to understanding the PET process using the theory calculations. Therefore, it is crucial to construct a simple model to investigate the mechanism of quinone-based PET from molecular level, which is not only for further understanding the natural PET process in photosystem II, but also for providing a significant reference for designing and synthesizing new PET-based molecules.

To reach this goal, we designed and synthesized a ubiquinone-based triphenylamine compound (TPA-CoQ<sub>0</sub>) to research the intramolecular PET from optical studies and Density Functional Theory (DFT) calculations. In TPA-CoQ<sub>0</sub>, triphenylamine and ubiquinone act as the simplest electron donor and electron acceptor, respectively. Ubiquinone undergoes two-step two-electron redox process, which could fine-tune the intramolecular PET process from triphenylamine moiety to ubiquinone group.

TPA-CoQ<sub>0</sub> was readily synthesized from one-step Suzuki Reaction between 6-Bormoubiquinone and 4-(diphenylamino) phenylboronic acid (Scheme 1). The <sup>1</sup>H and <sup>13</sup>C NMR, which are available in the ESI†, are consistent with its formulation. Single crystals of TPA-CoQ<sub>0</sub> suitable for the X-ray study were afforded via slow diffusion of petroleum ether into a dichloromethane solution of TPA-CoQ<sub>0</sub> at ambient temperature. An ORTEP drawing of the molecular structure of TPA-CoQ<sub>0</sub> (CCDC 1036959) is displayed in Fig. 1 and the full structural parameters are listed in the ESI†.



**Scheme 1.** The synthesis route of TPA-CoQ<sub>0</sub>.

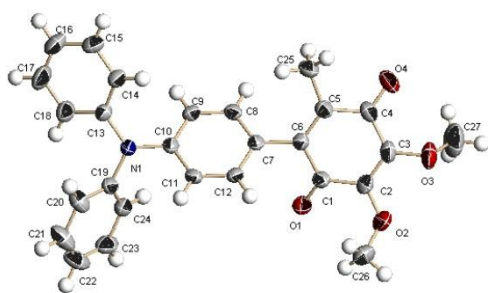


**Fig. 1** ORTEP representation of TPA-CoQ<sub>0</sub>. Where, blue = nitrogen, red = oxygen, gray = carbon, white = hydrogen.

To observe the fine-tuned PET between TPA and CoQ<sub>0</sub> as a result of ubiquinone redox process, the fluorescent and absorption spectra of TPA-CoQ<sub>0</sub> were measured as shown in Fig. 2, where NaBH<sub>4</sub> was used for ubiquinone reduction. TPA-CoQ<sub>0</sub> displays a non-fluorescence property (inset Fig. 2A) because the PET process took place between TPA group and CoQ<sub>0</sub> moiety. While, when NaBH<sub>4</sub> was added to reduce CoQ<sub>0</sub>, the TPA-H<sub>2</sub>CoQ<sub>0</sub> system exhibits a strong fluorescent at 515 nm (inset Fig. 2A). The appearance of the fluorescence is assigned to the blocked intramolecular PET from TPA to hydroquinone (H<sub>2</sub>CoQ<sub>0</sub>). The absorption spectra were measured to confirm the reduction of ubiquinone by NaBH<sub>4</sub>. As shown in Fig. 2B, TPA-CoQ<sub>0</sub> displays a strong and sharp absorption band at 299 nm and a weak and broad absorption band at 350–570 nm. The band at 299 nm is the overlapped result of the n- $\pi^*$  transition of the triphenylamine and the  $\pi$ - $\pi^*$  transition of the ubiquinonyl ring<sup>26, 27</sup>. The broad band is ascribed to the n- $\pi^*$  electronic transition of ubiquinonyl ring<sup>27</sup>. After addition of NaBH<sub>4</sub>, the broad band of TPA-CoQ<sub>0</sub> disappears indicating the n- $\pi^*$  electronic transition of ubiquinonyl ring is nonexistent and the CoQ<sub>0</sub> is reduced to H<sub>2</sub>CoQ<sub>0</sub>. These results reveal that the intramolecular PET would be control via the redox process of CoQ<sub>0</sub> group.

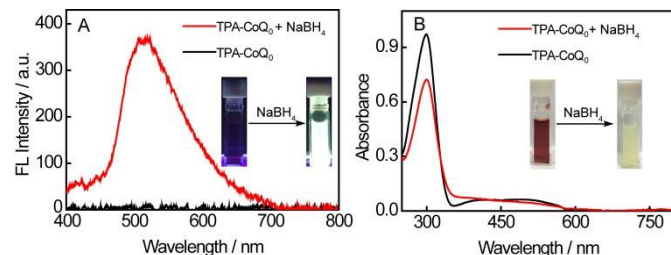


**Fig. 2** (A) Fluorescence and (B) absorption spectra of TPA-CoQ<sub>0</sub> (0.4 mM) in absence and presence of NaBH<sub>4</sub> in CH<sub>3</sub>CN. Inset: fluorescence and colour changes of TPA-CoQ<sub>0</sub> before and after adding NaBH<sub>4</sub>.

Next, the electrochemical and spectroelectrochemical properties of TPA-CoQ<sub>0</sub> were studied to further explore ubiquinone-tuned PET process. As can be seen from Fig. 3A, TPA-CoQ<sub>0</sub> exhibits three pairs of reversible redox peaks with the formal potentials at 0.949 V, -0.673 V and -1.349 V vs Ag/AgCl, respectively, which are consistent with the one electron redox process of TPA group and two electron redox processes of CoQ<sub>0</sub> moiety.<sup>27, 28</sup> Then, in situ UV-vis spectroelectrochemistry was measured to obtain the spectral information of TPA-CoQ<sub>0</sub> for investigating the fluorescent spectroelectrochemistry. As shown in the black and red lines of Fig. 3B, the broad absorption bands at 350–570 nm changed into a new band

at 380–470 nm with increasing intensity when applied a constant potential at -0.8 V, which indicated that ubiquinones were reduced to form semiquinone radicals. With the application of a more negative potential at -1.5 V, semiquinone anions were further reduced to dianionic and the disappeared n- $\pi^*$  absorption band of semiquinone radicals reveals ubiquinonyl ring totally is converted to aromatic ring<sup>29</sup>. The similar shapes of the red line in Fig. 2B and the blue line in Fig. 3B demonstrate the ubiquinone group could be completely reduced by NaBH<sub>4</sub> and electrochemical method.

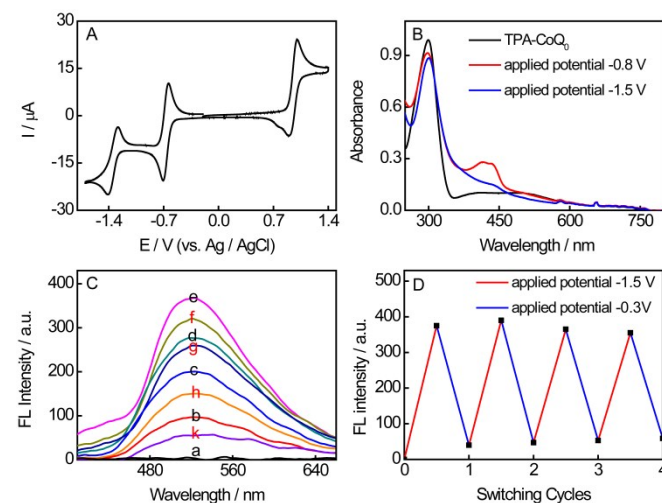


**Fig. 3** (A) CV curves of 1.0 mM TPA-CoQ<sub>0</sub> obtained at a glassy carbon electrode ( $\phi = 3$  mm) in anhydrous and deoxygenated CH<sub>3</sub>CN containing 0.1 M TBAP at scan rate 0.100 V s<sup>-1</sup>; (B) In situ UV-vis spectroelectrochemistry of 0.4 mM TPA-CoQ<sub>0</sub> obtained in an optically transparent electrochemical cell during the constant potential in aprotic CH<sub>3</sub>CN contained 0.1 M TBAP; (C) Fluorescence emission spectra changes of TPA-CoQ<sub>0</sub> with switched applied potentials, a-e: at the applied potential -1.5 V, e-k: at the applied potential -0.3 V; (D) Electrochemical fluorescence switched cycles with the redox cycle of TPA-CoQ<sub>0</sub>.

Fig. 3C displays the PL intensity changes of TPA-CoQ<sub>0</sub> at two switched applied potentials between -1.5 V and -0.3 V vs Ag/AgCl, where the ubiquinone moiety would be completely reduced or reoxidized. With the application of reduction potential at -1.5 V, a fluorescent signal occurs at 515 nm in the non-fluorescence TPA-CoQ<sub>0</sub> system and the PL intensity increases gradually along with the increasing time. While, when a constant potential at -0.3 V is applied, the decreased FL intensity is observed. The FL intensity changes of TPA-CoQ<sub>0</sub> is ascribed to the redox process of CoQ<sub>0</sub> group as observed using the NaBH<sub>4</sub> to reduce the CoQ<sub>0</sub> shown in Fig. 2A. Fig. 3D shows the electrochemical fluorescence switched cycles of TPA-CoQ<sub>0</sub> system upon the switched applied potentials between -1.5 V and -0.3 V. The FL intensity of TPA-CoQ<sub>0</sub> system increases during the electrochemical process with the constant potential at -1.5 V, indicating that the reduction of TPA-CoQ<sub>0</sub> takes place to lighten the system fluorescence. The FL intensity of the TPA-CoQ<sub>0</sub> system would gradually decreases with the reoxidation of reduced CoQ<sub>0</sub>. Additionally, the process is reversible and the FL intensity stays similar during the switched cycles due to the excellent electrochemical property of ubiquinone (Fig. 3D). These results demonstrate the redox process of CoQ<sub>0</sub> group could fine-tune the "off/on" and "on/off" fluorescence of the TPA-CoQ<sub>0</sub> system via switched the PET process.

To deeper illustrate the mechanism process, Density Functional Theory (DFT) for the first time was used in ubiquinone-base PET system to understand the PET process from the molecular basis and attempt to provide a theory model, where polarizable continuum model (PCM) was used for describing the solvent and the interaction between solvent and solutes.

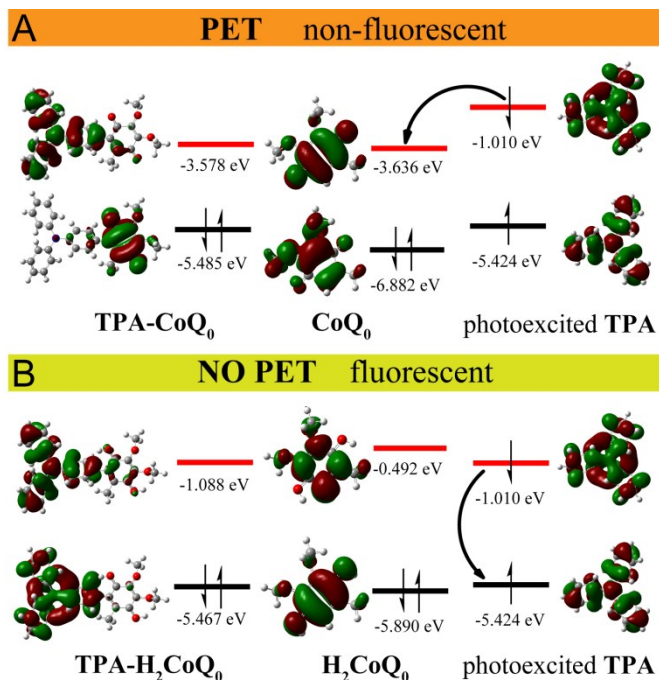


**Fig. 4** The frontier molecular orbital energy diagrams of (A) TPA-CoQ<sub>0</sub>, CoQ<sub>0</sub>, photoexcited TPA, and (B) TPA-H<sub>2</sub>CoQ<sub>0</sub>, H<sub>2</sub>CoQ<sub>0</sub>, calculated at the B3LYP/6-311++G(d, p) level of theory in CH<sub>3</sub>CN (Red line: LUMO; Black line: HOMO). Polarizable continuum model (PCM) was used for describing the solvent and the interaction between solvent and solutes.

As shown in Fig. 4A, the LUMO and HOMO of TPA-CoQ<sub>0</sub> are localized on TPA group and CoQ<sub>0</sub> group, which are ascribed to the fact that TPA and CoQ<sub>0</sub> act as an electron donor and an electron acceptor in TPA-CoQ<sub>0</sub> system, respectively. In addition, the LUMO energy level of TPA-CoQ<sub>0</sub> is consistent with that of CoQ<sub>0</sub>, while the HOMO energy level of TPA-CoQ<sub>0</sub> is in good agreement of that of TPA. The energy levels of TPA-CoQ<sub>0</sub> could be contributed to a weak orbital communications as a result of the large dihedral angle (55.84°) between CoQ<sub>0</sub> moiety and TPA moiety obtained from DFT calculations using CH<sub>3</sub>CN as solvent.<sup>28</sup> The PET process would be explained clearly from the frontier molecular orbital energy diagrams shown in Fig. 4. As can be seen from the Fig. 4A, in the oxidation state of CoQ<sub>0</sub> moiety, the LUMO of CoQ<sub>0</sub> (-3.636 eV) is lower than that of TPA (-1.010 eV) and the HOMO of TPA (-5.424 eV) is higher than that of CoQ<sub>0</sub> (-6.882 eV). Therefore, when electrons of TPA is excited from its HOMO to LUMO, the electrons would be back to the LUMO of CoQ<sub>0</sub> rather than HOMO of TPA and the HOMO electrons of CoQ<sub>0</sub> also would not inject into HOMO of TPA. The intramolecular PET from the photoexcited LUMO of TPA to LUMO of CoQ<sub>0</sub> lets non-fluorescence property of TPA-CoQ<sub>0</sub>. However, when CoQ<sub>0</sub> group is reduced to H<sub>2</sub>CoQ<sub>0</sub>, the LUMO of H<sub>2</sub>CoQ<sub>0</sub> (-0.492 eV) would be higher than that of TPA (-1.010 eV) and the HOMO of H<sub>2</sub>CoQ<sub>0</sub> (-5.890 eV) still

is lower than the HOMO of TPA (-5.424 eV) as shown in Fig. 4B. In this case, the photo-excited electron of TPA would return to its HOMO and the photons are released. The blocked PET makes the system displays a strong fluorescence. The DFT calculations reveal that the nature of the switched intramolecular PET process is ascribed to the changed molecular orbitals of CoQ<sub>0</sub> during its redox process. The picture of the intramolecular PET becomes clear that the efficient PET system should occupy the matched molecular orbitals between the donor and acceptor groups, which could be obtained from the inchoate DFT calculations before we synthesize new PET-based molecules. The fine-tuned PET process of TPA-CoQ<sub>0</sub> model provides a DFT-based reference for designing new molecules with efficient PET.

In conclusion, a ubiquinone-based triphenylamine compound was synthesized as a simple model to study the photo-induced electron transfer (PET). The optical studies indicate the PET process could be fine-tuned via redox of ubiquinone and the system exhibits "off/on" and "off/on" fluorescent properties between TPA-CoQ<sub>0</sub> and TPA-H<sub>2</sub>CoQ<sub>0</sub>. The DFT calculations also demonstrate that the changed LUMO orbitals of ubiquinone/hydroquinone are ascribed to the switched PET processes. These results suggest that suitable molecular structures with efficient PET property could be calculated before synthesizing and would give excellent properties for their applications in artificial photosynthesis systems or sensors. This work provides a simple theory model for deeper insight into the intramolecular PET and would give a fundamental reference for new PET-based molecules development.

This work is supported by the National Science Fund of China (21327807), the National Based Research 973 Program (2013CB733700) and Science Fund for Creative Research Groups (21421004). Y.T.Long is supported by the National Science Fund for Distinguished Young Scholars of China (21125522) and Shanghai Pujiang Program (12JC1403500).

## Notes and references

Key Laboratory for Advanced Materials & Department of Chemistry, East China University of Science and Technology, 130 Meilong Road, Shanghai, 200237, P. R. China. \*E-mail: ytlong@ecust.edu.cn

† Electronic Supplementary Information (ESI) available: [General methods of experiments, synthesis and structure characterizations of compounds, additional single crystal data]. See DOI: 10.1039/b000000x/

1. R. Emerson, R. Chalmers and C. Cederstrand, *Proc. Natl. Acad. Sci. U. S. A.*, 1957, **43**, 133-143.
2. M. Nonella, *J. Phys. Chem. B*, 1998, **102**, 4217-4225.
3. A. Bauer, F. Westkamper, S. Grimme and T. Bach, *Nature*, 2005, **436**, 1139-1140.
4. Y. Ooyama, A. Matsugasako, K. Oka, T. Nagano, M. Sumomogi, K. Komaguchi, I. Imae and Y. Harima, *Chem Commun*, 2011, **47**, 4448-4450.
5. F. Yu, P. Li, G. Li, G. Zhao, T. Chu and K. Han, *J. Am. Chem. Soc.*, 2011, **133**, 11030-11033.
6. F. Yu, P. Li, P. Song, B. Wang, J. Zhao and K. Han, *Chem Commun*, 2012, **48**, 4980-4982.
7. M. H. Lee, B. D. Dunietz and E. Geva, *J. Phys. Chem. C.*, 2013, **117**, 23391-23401.
8. J. J. Shie, Y. C. Liu, Y. M. Lee, C. Lim, J. M. Fang and C. H. Wong, *J. Am. Chem. Soc.*, 2014, **136**, 9953-9961.

9. K. Stranius, V. Iashin, T. Nikkonen, M. Muuronen, J. Helaja and N. Tkachenko, *J. Phys. Chem. A*, 2014, **118**, 1420-1429.
10. L. Yuan, W. Lin, K. Zheng, L. He and W. Huang, *Chem. Soc. Rev.*, 2013, **42**, 622-661.
11. M. D. Peterson, R. J. Holbrook, T. J. Meade and E. A. Weiss, *J. Am. Chem. Soc.*, 2013, **135**, 13162-13167.
12. H. Zhu, J. Fan, J. Wang, H. Mu and X. Peng, *J. Am. Chem. Soc.*, 2014, **136**, 12820-12823.
13. F. Cailliez, P. Muller, M. Gallois and A. de la Lande, *J. Am. Chem. Soc.*, 2014, **136**, 12974-12986.
14. C. F. B. Dias, J. C. Araújo-Chaves, K. C. U. Mugnol, F. J. Trindade, O. L. Alves, A. C. F. Caires, S. Brochsztain, F. N. Crespilho, J. R. Matos, O. R. Nascimento and I. L. Nantes, *RSC Advances*, 2012, **2**, 7417.
15. B. Tong, H. Yang, W. Xiong, F. Xie, J. Shi, J. Zhi, W. K. Chan and Y. Dong, *J. Phys. Chem. B*, 2013, **117**, 5338-5344.
16. X. Zhang, Y. Zeng, T. Yu, J. Chen, G. Yang and Y. Li, *J. Phys. Chem. Lett.*, 2014, **5**, 2340-2350.
17. A. Magnuson, H. Berglund, P. Korall, L. Hammarström, B. Åkermark, S. Styring and L. Sun, *J. Am. Chem. Soc.*, 1997, **119**, 10720-10725.
18. L. Sun, M. Burkitt, M. Tamm, M. K. Raymond, M. Abrahamsson, D. LeGourriérec, Y. Frapart, A. Magnuson, P. H. Kenč, P. Brandt, A. Tran, L. Hammarström, S. Styring and B. Åkermark, *J. Am. Chem. Soc.*, 1999, **121**, 6834-6842.
19. O. S. Wenger, *J. Am. Chem. Soc.*, 2012, **134**, 12844-12854.
20. G. Steinberg-Yfrach, J.-L. Rigaud, E. N. Durantini, A. L. Moore, D. Gust and T. A. Moore, *Nature*, 1998, **392**, 479-482.
21. S. L. Gould, G. Kodis, R. E. Palacios, L. de la Garza, A. Brune, D. Gust, T. A. Moore and A. L. Moore, *J. Phys. Chem. B*, 2004, **108**, 10566-10580.
22. L. X. Qin, W. Ma, D. W. Li, Y. Li, X. Chen, H. B. Kraatz, T. D. James and Y. T. Long, *Chem. Eur. J.*, 2011, **17**, 5262-5271.
23. W. C. Silvers, B. Prasai, D. H. Burk, M. L. Brown and R. L. McCarley, *J. Am. Chem. Soc.*, 2013, **135**, 309-314.
24. W. Ma, L. X. Qin, F. T. Liu, Z. Gu, J. Wang, Z. G. Pan, T. D. James and Y. T. Long, *Scientific reports*, 2013, **3**, 1537.
25. S. U. Hettiarachchi, B. Prasai and R. L. McCarley, *J. Am. Chem. Soc.*, 2014, **136**, 7575-7578.
26. Y. Tao, Q. Wang, L. Ao, C. Zhong, J. Qin, C. Yang and D. Ma, *J. Mater. Chem.*, 2010, **20**, 1759.
27. W. Ma, H. Zhou, Y.-L. Ying, D.-W. Li, G.-R. Chen, Y.-T. Long and H.-Y. Chen, *Tetrahedron*, 2011, **67**, 5990-6000.
28. S. Tang, W. Li, F. Shen, D. Liu, B. Yang and Y. Ma, *J. Mater. Chem.*, 2012, **22**, 4401-4408.
29. M. Bauscher and W. Maentele, *J. Phys. Chem.*, 1992, **96**, 11101-11108.